

Benchmarking Residual Dose Rates in a NuMI-like Environment*

I. Rakhno[†], N. Mokhov, A. Elwyn, N. Grossman, and K. Vaziri
Fermi National Accelerator Laboratory, Batavia, Illinois 60510-0500, USA

M. Huhtinen
CERN, Geneva, CH-1211, Switzerland

and

L. Nicolas
University of Orsay, Paris, France

Abstract – *Activation of various structural and shielding materials is an important issue for many applications. A model developed recently to calculate residual activity of arbitrary composite materials for arbitrary irradiation and cooling times is presented in the paper. Measurements have been performed at the Fermi National Accelerator Laboratory to study induced radioactivation of different beam line components and shielding materials. The calculated residual dose rates for the samples studied are presented and compared with the measured ones.*

I. INTRODUCTION

An important issue regarding the radiation environment in the NuMI complex of the MINOS neutrino experiment, currently under construction at Fermi National Accelerator Laboratory¹, is induced radioactivation of the beam line components and shielding materials. This arises from irradiation by hadrons that are generated in the target bombarded by a 120 GeV proton beam. The MARS Monte Carlo code² is used to predict and analyse prompt and residual radiation in such an environment. New modules have been developed for the MARS14 version for reliable estimation of residual dose rates in arbitrary composite materials for arbitrary irradiation and cooling times. The algorithm distinguishes three major energy groups responsible for radionuclide production: above 20 MeV, 1 to 20 MeV and a thermal neutron group (under 0.5 eV). To understand the properties of the residual radiation and benchmark the newly developed code modules, measurements were performed both in the vault area and at a location just outside the steel shielding at the antiproton (AP0) target area, which is thought to be a realistic representation of the NuMI target area. All the details of the AP0 enclosure (in-vault and the outer shielding) and the appropriate beam line components were built in the MARS calculation model

and detailed simulations were performed. Calculated residual dose rates and neutron spectra are compared with the data showing good agreement.

II. EXPERIMENTAL SETUP

A MARS model of the experimental setup is shown in Fig. 1. Residual activation exposure rates were measured for five small cylindrical and rectangular samples of iron, steel, aluminum, and concrete, which were obtained from materials that will be used in the NuMI construction. Composition of the samples is described in Table I. The samples were placed both within the vault area (just down stream of the antiproton production target) and at a location just outside of the steel shielding at AP0. Further, thin activation foils of Au, Au+Cd, In, and Al were mounted on a disk and placed at both locations. The neutron spectra were unfolded from measured foil activities by use of response functions determined from known cross section data with the unfolding codes BUNKI and LOUHI³. The samples within the vault were irradiated for a total of 38 hours by the radiation arising from the bombardment of the target by about 1.3×10^{17} 120 GeV protons from the Main Injector, and then removed to a low background area for counting; those outside of the shielded vault area were irradiated on and off for about four months with a total of approximately 3.6×10^{18} protons incident on the in-vault target. Background corrected exposure rates of the samples were determined by use of both GM and NaI scintillator based survey instruments.

III. CALCULATIONAL MODEL

III.A. Model for residual dose rate estimation

The model developed for residual dose rate calculation introduces a relationship between density of inelastic nuclear interactions (or, in other words, stars) and the residual dose rate. Quantitatively the relationship is expressed by means of the so-called ω -factors which depend on type and duration of the

* Work supported by the Universities Research Association, Inc., under contract DE-AC02-76CH03000 with the U.S. Department of Energy.

[†] rakhno@fnal.gov

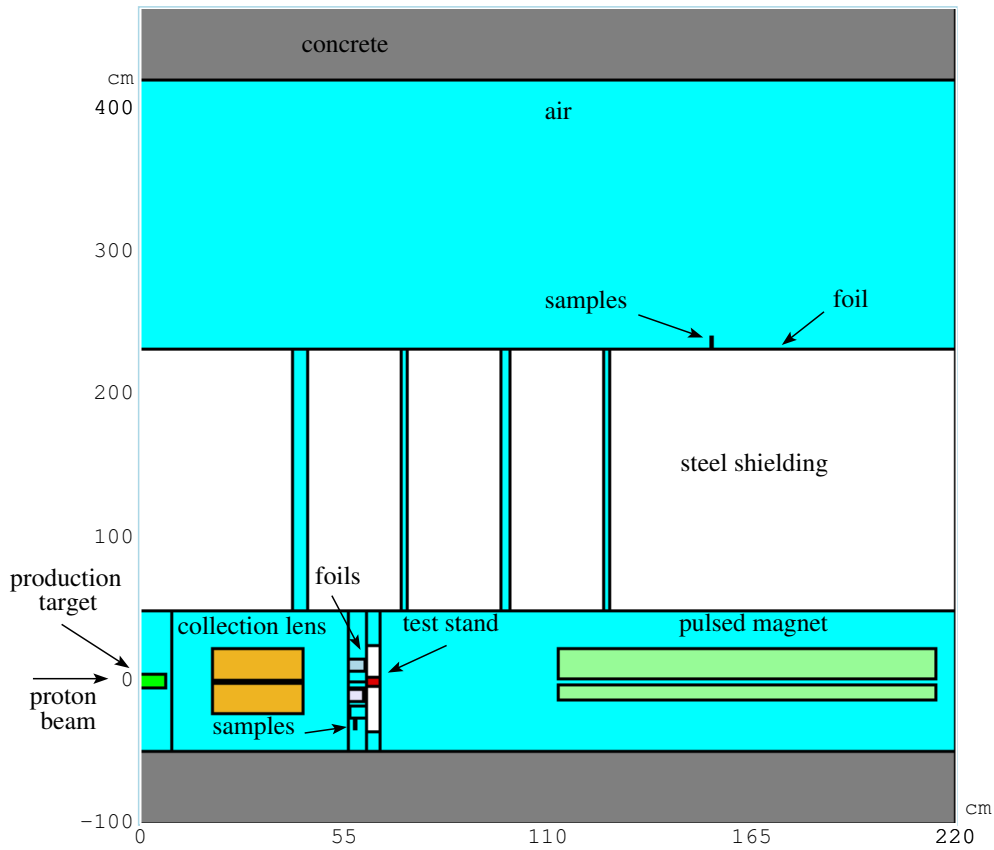


Fig. 1. Elevation view of the experimental area as modeled in MARS.

TABLE I. Composition of the samples investigated (weight %)

Sample (label)	Nuclide (or natural mixture)													
	^1H	^{12}C	^{16}O	^{23}Na	Mg	^{27}Al	Si	S	K	Ca	^{55}Mn	Fe	Ni	Cu
1 (Aluminum)						100								
2 (Iron)		0.1					0.1				0.4	98.2	1.0	0.2
3 (1018 Steel)		0.2									0.9	98.9		
4 (Concrete ^a)	0.8	7.3	51.76	0.07	6.5	0.5	10.1	0.2	0.07	21.1		1.6		
5 (A500 Steel)		0.3										99.5		0.2

^aPrecise composition of the concrete sample is not presently known. This Table shows the reference composition used.

irradiation as well as on subsequent cooling. Detailed description of the model will be given elsewhere. As an example, numerical values of the ω -factors for neutron irradiation at typical conditions (30 days irradiation and 1 day cooling) are presented in Fig. 2.

III.B. Coupling MARS with MCNP

In the current MARS version² the MCNP4C code⁴ is invoked whenever a low-energy (under 14.5 MeV) neutron collision with matter is simulated. However, when considering problems with dominating low-energy neutron radiation, the full-scale MCNP modeling of neutron transport in matter is preferable for the following reasons: (i) different built-in vari-

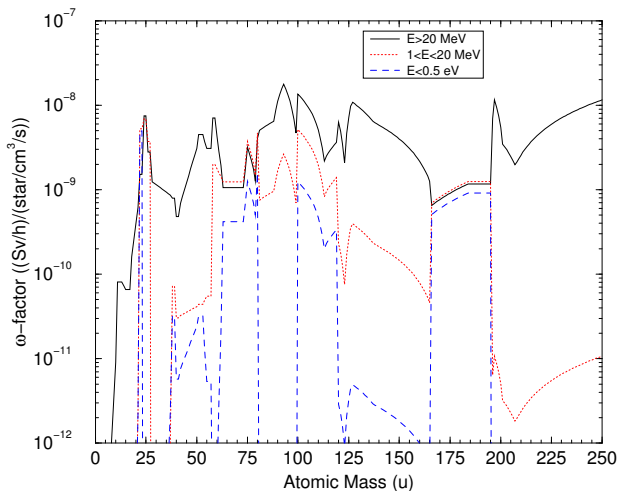


Fig. 2. The ω -factors for different neutron energies vs mass of a target nucleus.

ance reduction techniques can be used; (ii) neutron flux functionals characteristic of the low-energy region that take into account the detailed energy dependence of neutron cross sections are readily available. That is why another option for MARS-to-MCNP coupling was developed recently (such an option is used for coupling high- and low-energy parts in other codes as well⁵). Namely, when modeling neutron transport with the MARS code, instead of low-energy neutron tracking, one can generate a file containing all the necessary phase-space coordinates for all the neutrons slowed-down to energies under 14.5 MeV. The file can be used as a neutron source for subsequent standalone MCNP modeling.

It will be shown in the following sections that in the in-vault region at the location of the thin foils the calculated neutron spectrum has a low-energy part (under 10 MeV) that amounts to 90%. As for above the vault shielding, the calculated neutron spectra do not contain neutrons with energies above 10 MeV within the simulation statistics. This is *a posteriori* justification of the importance of the option for low-energy neutron transport used in the calculations described.

III.C. Dose rate attenuation factors

Measurement of the residual dose rate for a sample can be performed both on contact and at a distance. To have a simple and easy-to-use relationship when comparing measured or calculated contact dose rate with that at a distance (typically at 30.5 cm), calculations with the MCNP code⁴ have been performed. Two types of samples were taken into consideration; namely, cylinders and parallelepipeds of the same radii (1.27 cm) and thicknesses (2.54 cm), respectively, but with other dimensions being different. Several material compositions were used in the study. Residual activity of the samples was simulated by means of gammas born with isotropic angular distribution and spatially uniform over a sample volume. Monoenergetic

1-MeV gammas were considered; this adequately represents the average energy of gammas emitted from different irradiated concrete or steel samples.

Both contact and remote dose rates were determined as average values over surface segments with linear dimension equal to one inch. One of the segments was located on a surface of a sample under consideration, the second one at different distances from the sample. The ANSI/ANS-6.1.1-1977 table⁴ was used to convert the calculated photon fluxes over the segments to dose rates. The dose rate attenuation factor for a definite distance from a sample surface was determined as the ratio of the calculated dose rates for the two segments at that distance. The calculated factors were fitted by means of a d^α function using χ^2 criterion, where d is the distance from the surface of the sample under consideration, and α is the fitted parameter. Typical behaviour of the attenuation factors is presented in Fig. 3.

IV. RESULTS AND DISCUSSION

IV.A. Residual dose rates

Comparison between measured and calculated residual dose rates for the samples near beam and above the steel shielding is presented in Figs. 4 through 6. In general, good agreement is observed for the near-beam irradiations (Fig. 4); the agreement is good in shape and within factors of 2-5 in magnitude. The residual dose rates were calculated taking into account realistic non-continuous in time irradiation (three sessions, 16.2, 10.5, and 11 hours long, separated by different beam-off periods) as well as measured integrated proton intensities on the target. For above shielding irradiations (Fig. 5), approximately 16 hours of beam-on was followed by 26 hours of beam-off on the average during the irradiation period of four months. That non-continuous irradiation was taken into account in our calculations as well. One can see that the agreement is good for cooling times greater than one day. The discrepancy for shorter times is probably due to inadequate description in our model of short-lived radionuclides which would be observed. In this case, following the last beam-on period, counting was started within two hours so that significant short-lived radionuclide activities would be observed.

Significant discrepancy observed for concrete samples (Fig. 6) requires additional investigation. According to our model, the calculated residual dose rate for the samples is very sensitive to the composition of the concrete. As an example, calculated residual dose rates above the steel shielding for different concrete sample compositions available are shown in Table II. As observed, small differences in composition can lead to significant differences in calculated dose rates (up to factors of about 50). We attribute this effect mainly to minor admixtures in the region of Na (see Figs. 2 and 7). Since we do not know exactly the composition of the concrete samples (with regard to minor admixtures) used in these studies, the discrepancy between calculations and measurements may not

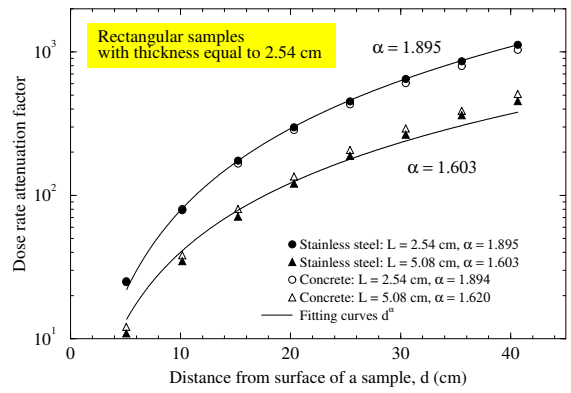
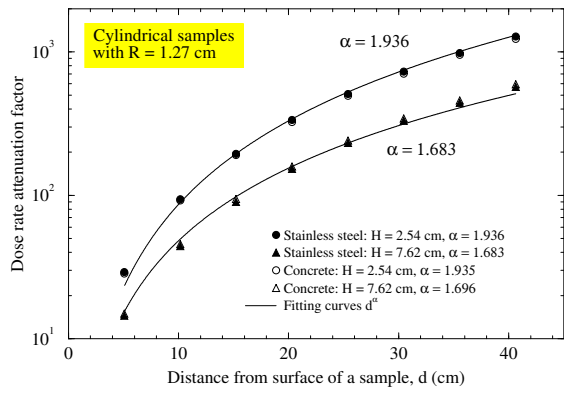


Fig. 3. Calculated surface dose rate attenuation factors for different samples.

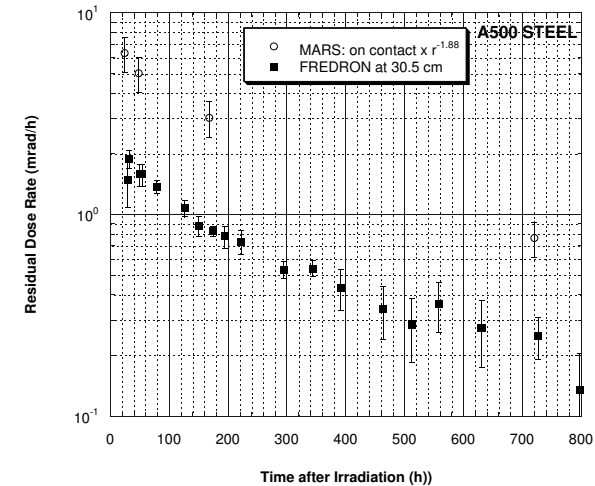
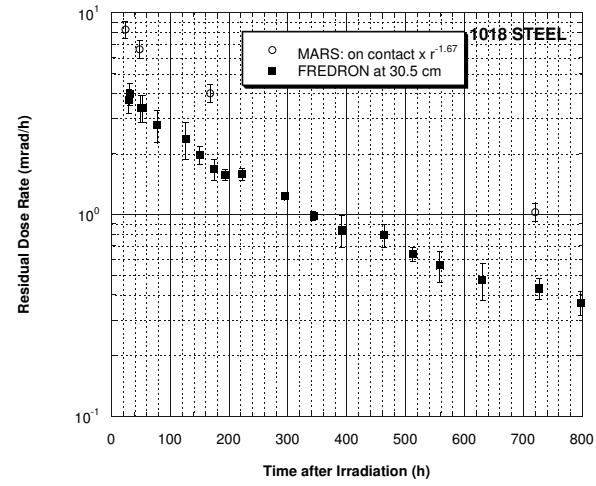
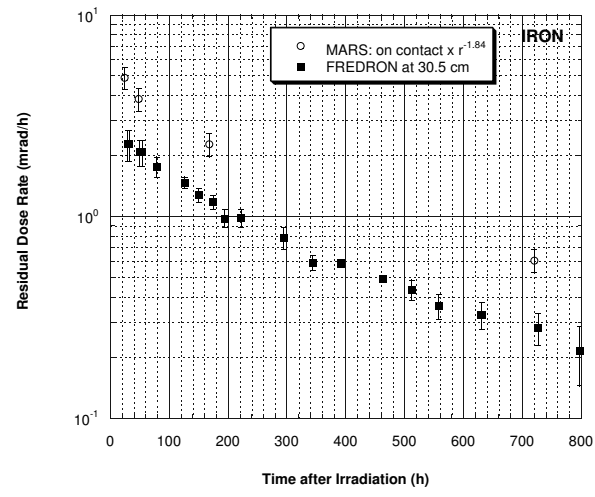
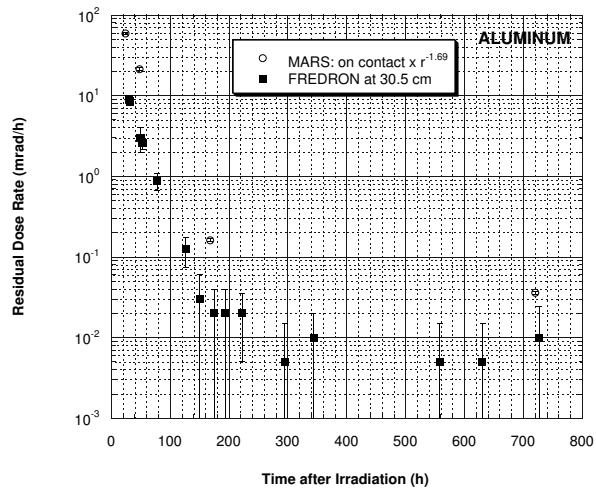


Fig. 4. Measured (FREDRON) and calculated (MARS) residual dose rate at $d = 30.5\text{cm}$ for the samples irradiated for 38 hours near beam vs cooling time.

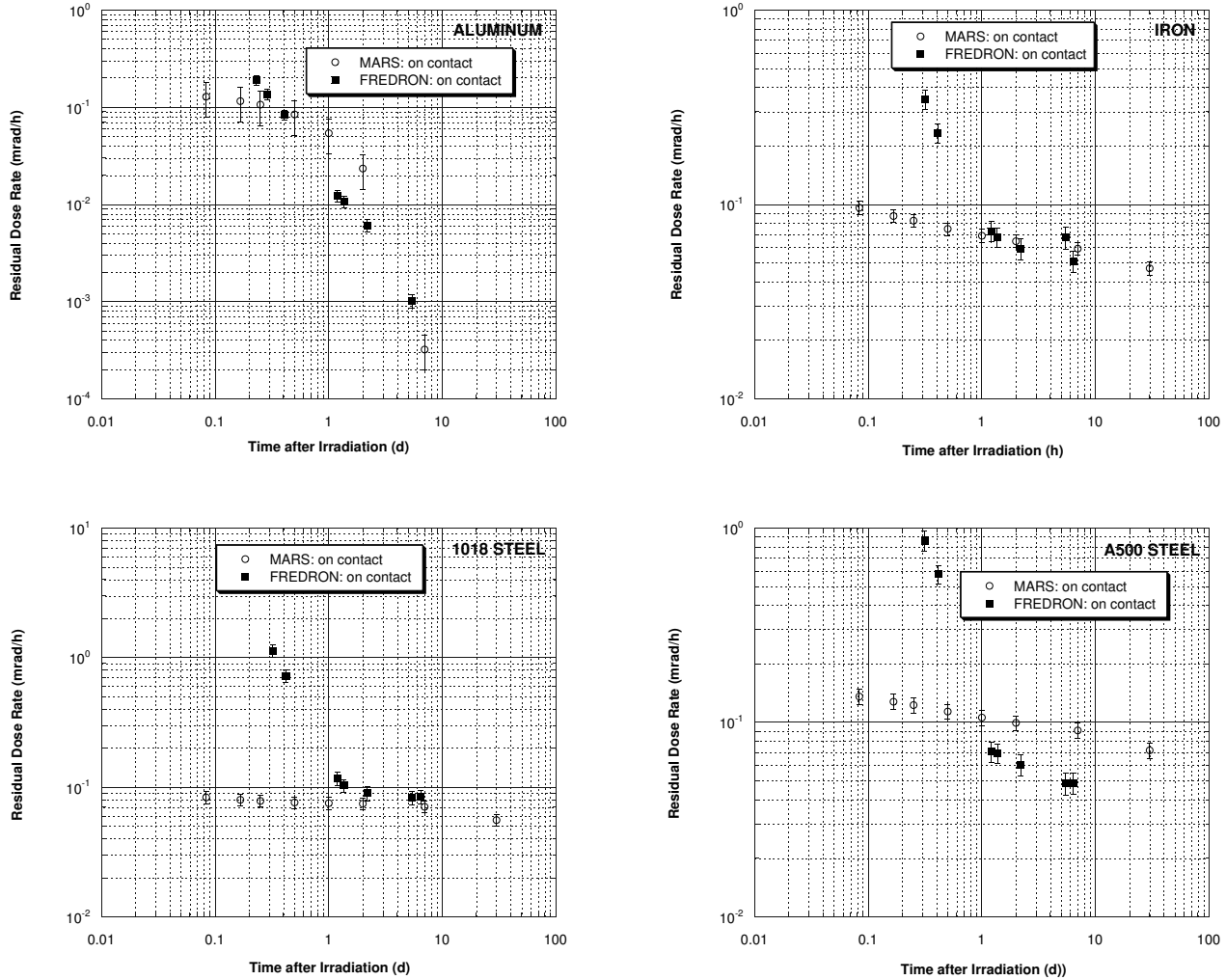


Fig. 5. Measured (FREDRON) and calculated (MARS) residual dose rate on contact for the samples irradiated for four months over the shielding vs cooling time.

be unexpected.

IV.B. Neutron spectra

Calculated neutron spectra near beam and above the shielding as well as unfolded spectra near beam based on measured foil activities are presented in Fig. 7. Location of the foils is shown in Fig. 1. One can see that even for the foils near-beam the low-energy part of the neutron spectrum dominates. Above the vault shielding the spectrum, within the simulation statistics, does not reveal neutrons with energies above 10 MeV. In addition, one can see that in this location neutrons backscattered from the concrete walls and ceiling dominate. This backscattered component is especially important for the two lower energy groups (under 0.5 eV and from 1 up to 20

MeV) responsible for formation of induced radioactivity according to our model. It means that for the location above the shielding one could not predict residual dose rates correctly without taking into account neutron backscattering from the concrete surroundings.

The neutron spectrum within the vault was unfolded from measured radioactivity of Au and In foils. The response functions used in the unfolding codes BUNKI and LOUHI³ were determined at eight rather broad energy bins in order to cover the neutron energy range up to 70 MeV. Therefore, at energies below 0.1 MeV, the unfolded spectrum represents a broad average, and this gives little quantitative information in comparison with the more detailed spectrum calculated with the MARS code. At energies above 0.1 MeV, however, acceptable agreement between calculations and measurements is ob-

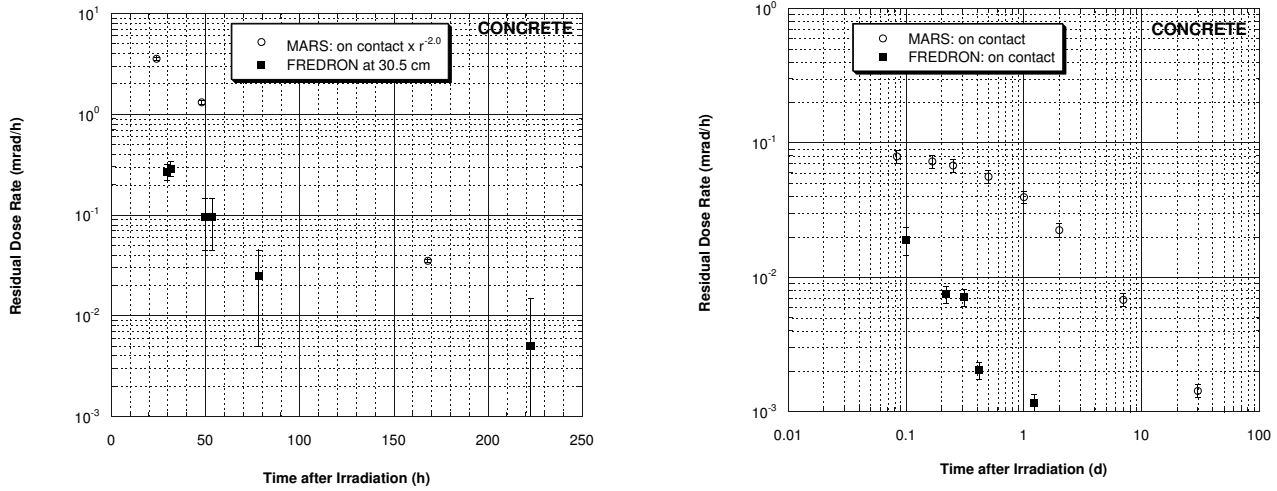


Fig. 6. Measured (FREDRON) and calculated (MARS) residual dose rate for the concrete samples irradiated for 38 hours near beam (left) and four months over the shielding (right) vs cooling time. The dose rates were measured at $d = 30.5\text{cm}$ and on contact, respectively.

TABLE II. Calculated residual dose rates (0.01 mSv/hr) for different compositions (weight %) of the concrete sample above the shielding. The data were obtained for 30 days irradiation at 10^{12} protons per second and 1 day cooling.

Concrete composition	Nuclide (or natural mixture)											Dose rate
	^1H	^{12}C	^{16}O	^{23}Na	Mg	^{27}Al	Si	S	K	Ca	Fe	
1	0.6		49.8	1.7	0.3	4.6	31.5		1.9	8.3	1.3	1.7
2	0.6	3.0	50.0	1.0		3.0	20.0		1.0	20.0	1.4	1.0
3	0.8	7.3	51.76	0.07	6.5	0.5	10.1	0.2	0.07	21.1	1.6	0.09
4	0.5	6.4	49.6		1.0	1.5	14.3	0.2		26.1	0.4	0.03

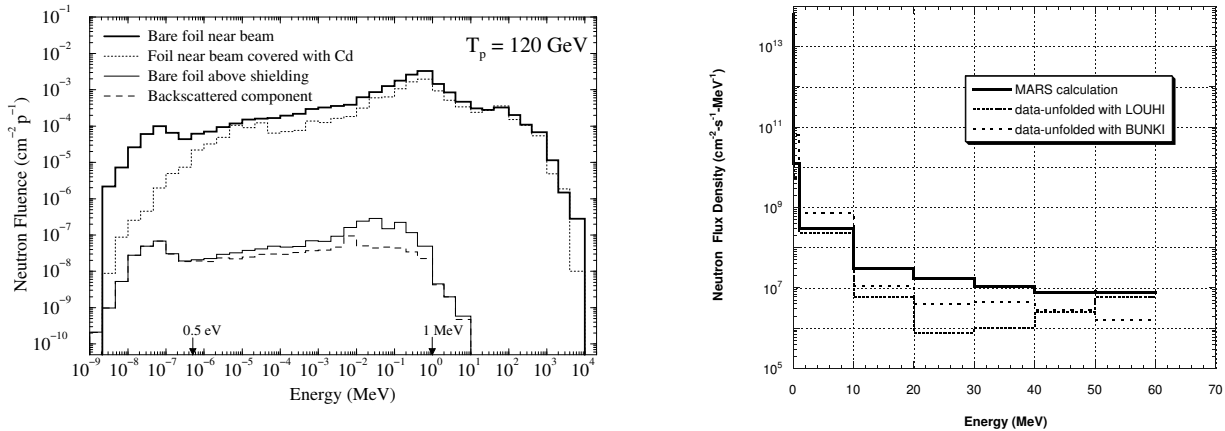


Fig. 7. Calculated (by means of the MARS and MCNP codes) neutron spectra near beam and above the shielding (left) as well as unfolded spectra near beam (right). Normalization was performed per one incident proton (left) and 10^{12} protons per second (right).

served, as seen in Fig. 7.

V. CONCLUDING REMARKS

The model was developed for calculation of residual dose rates in arbitrary composite materials for arbitrary irradiation and cooling times. Measurements have been performed at Fermi National Accelerator Laboratory on induced radioactivation of beam line components and shielding materials. Reasonable agreement is observed between measured and calculated dose rates for different samples irradiated at different conditions. At the same time significant disagreement is observed for concrete samples which reveal high sensitivity of calculated residual dose rate to content of minor admixtures in concrete. The disagreement is a subject of our further investigations.

ACKNOWLEDGMENT

It is a pleasure to thank A. Wehmann of Fermilab for helpful discussions on subjects covered in the paper.

REFERENCES

1. K. ANDERSON, B. BERNSTEIN, D. BOEHNLEIN, *et al.*, "The NuMI Facility Technical Design Report", Revision 1.0, October 1998, FNAL (1998).
2. N. V. MOKHOV, "The MARS Code System User's Guide", Fermilab-FN-628 (1995); N. V. MOKHOV and O. E. KRIVOSHEEV, "MARS Code Status", Fermilab-Conf-00/181 (2000). <http://www-ap.fnal.gov/MARS/>.
3. K. LOWRY and T. JOHNSON, "Modification to Iterative Recursion Unfolding Algorithms and Computer Codes to Find More Appropriate Neutron Spectra", US Naval Research Laboratory, Report NRL-5340 (1984); J. T. ROUTTI and J. V. SANDEBERG, "General Purpose Unfolding LOUHI78 with Linear and Non-Linear Regularization", *Comp. Phys. Comm.*, **21**, 119 (1980).
4. J. F. BRIESMEISTER, editor, "MCNP - A General Monte Carlo N-Particle Transport Code", Version 4C. Pub. LA-13709-M, LANL (2000).
5. R. E. PRAEL and H. LICHTENSTEIN, "User Guide to LCS: The LAHET Code System", Pub. LA-UR-89-3014, LANL (1989).